22PFL-0652

Development of an Adaptive Efficient Thermal / Electric Skipping Control Strategy applied to a parallel plug-in hybrid electric vehicle

Author, co-author (Do NOT enter this information. It will be pulled from participant tab in MyTechZone)

Affiliation (Do NOT enter this information. It will be pulled from participant tab in MyTechZone)

Abstract

In recent years automobile manufacturers focused on an increasing degree of electrification of the powertrains with the aim to reduce pollutants and CO_2 emissions. Despite more complex design processes and control strategies, these powertrains offer improved fuel exploitation compared to conventional vehicles thanks to intelligent energy management. A simulation study is here presented aiming at developing a new control strategy for a P3 parallel plug-in hybrid electric vehicle. The simulation model is implemented using vehicle modeling and simulation toolboxes in MATLAB/Simulink. The proposed control strategy is based on an alternative utilization of the electric motor and thermal engine to satisfy the vehicle power demand at the wheels (Efficient Thermal/Electric Skipping Strategy - ETESS). The choice between the two units is realized through a comparison between two equivalent fuel rates, one related to the thermal engine and the other related to the electric consumption. An adaptive function is introduced to develop a charge-blended control strategy. The novel adaptive control strategy (A-ETESS) is applied to estimate fuel consumption along different driving cycles. The control algorithm is implemented on a dedicated microcontroller unit performing a Processor-In-the-Loop (PIL) simulation. To demonstrate the reliability and effectiveness of the A-ETESS, the same adaptive function is built on the Equivalent Consumption Minimization Strategy (ECMS). The PIL results showed that the proposed strategy ensures a fuel economy similar to ECMS (worse of about 2% on average) and a computational effort reduced by 99% on average. This last feature reveals the potential for real-time on-vehicle applications.

Introduction

Electrified powertrains are one of the key technologies for vehicle energy saving. Combining an Internal Combustion Engine (ICE) and one or more high-efficiency electric machines, Hybrid Electric Vehicles (HEVs) have lower fuel consumption than conventional vehicles. However, effective Energy Management Strategies (EMSs) are required to coordinate the energy distribution among powertrain components and, at the same time, respecting their safe working condition.

Zhang et al. [1] proposed to classify EMSs in two main headlines: (1) offline EMSs, categorized according to the information level of the driving conditions utilized, including global optimization based-EMSs and rule-based EMSs; and (2) online EMSs represented as instantaneous optimization-based EMSs, predictive EMSs, and learning-based EMSs.

Offline EMSs are mainly divided into global optimization-based EMSs and rule-based EMSs. Rule-based EMSs are based on the selection of driving modes. They are typically used in real-time applications thanks to their low computational effort. [2,3,4]. Dynamic programming (DP) and Pontryagin Minimization Principle (PMP) are two of the most common offline EMSs. DP is a mathematical technique to find the global optimum solution in managing the energy sources in hybrid power trains [5,6]. Therefore, it is used as a benchmark tool for other EMSs [7]. It requires prior knowledge of the entire driving cycle and has high computational complexity. PMP is an analytical optimization method that transforms a global optimization problem into an instantaneous Hamiltonian optimization problem [8,9]. Its main disadvantage is the requirement of the co-state estimation [10,11]. Kim et al. [12] developed a methodology to calculate the optimal co-state when a driving cycle is given. The simulation results showed that PMP control can achieve near-optimal results compared to DP. The computational time for PMP-based control was a tenth of that for DP-based control.

The Equivalent Consumption Minimization Strategy (ECMS) can be considered a PMP extension for online implementation. It is based on the idea that power is distributed by minimizing the fuel consumption at each instant by converting the electricity consumption into the equivalent fuel consumption. [13,14] The control variable in EMCS is an Equivalent Factor (EF) that relates the electric energy consumption to the power requirement. Wang et al. [15] developed a real-time ECMS for a series-parallel hybrid electric bus. HIL simulations showed that the proposed Adaptive ECMS (A-ECMS) can reduce the fuel consumption of the hybrid bus by 12.75% and 40.57% compared to the hybrid electric bus with a logic-threshold control strategy and the conventional ICE bus, respectively.

State of Charge (SoC) management strategies are classified according to how the SoC of the energy storage system varies with time. Hybrid Electric Vehicles (HEVs) cannot charge the battery from the grid so, Charge-Sustaining (CS) strategies are developed aiming to keep the SoC level around a predefined target. Plug-in HEVs (PHEVs) could have the potential for providing pure electric driving for a longer range (with respect to HEVs) and CS strategies are not appropriate. Charge-Depleting (CD)/Charge-Sustaining strategies consist of a plan that firstly discharges the battery until a certain SoC level and then sustains the SoC around the above level. [16,17]. They are widely implemented in heuristic hybrid control modules of PHEVs [18,19]. Charge Blended

(CB) strategies are similar to CS strategies, but the SoC target decreases linearly with the driven distance [20]. CB strategies are compatible with PHEVs that usually start driving missions with a fully charged battery and aim to arrive with a lower SoC level at the end of the mission. It is widely recognized that, in CB mode, the ICE operates in its most efficient region longer, resulting in lower CO_2 emissions [21]. Several approaches have been proposed in the literature to realize adaptive CB control strategies [22, 23, 24]. In [25] the authors developed an artificial neural network-enhanced ECMS for a PHEV. Results highlight a reduced energy total cost compared to a simple CD-CS strategy for each test case, however computational time is more than 10 times increased. Onori et al. [26, 27] designed a causal controller PMP based to develop a CB strategy. The adaption law was tuned and implemented in a vehicle model in the form of a look-up table, where the optimal value of the co-state is tabulated as a function of total traveled distance and average driving cycle speed. Simulation results were compared to PMP and CD/CS mode, and they showed that the proposed strategy can improve fuel consumption by around 20%. On the other hand, PMP require higher computational effort compared to CD/CS approach, as shown in [25].

To reduce computational time typical of ECMS strategies, in previous work of the authors [28] a simplified control strategy was proposed, based on an alternative utilization of the thermal and electric unit for the vehicle driving (Efficient Thermal Electric Skipping Strategy – ETESS). At each time the choice between the power source depends on the comparison between the actual fuel rate in pure ICE driving and an equivalent fuel rate in pure electric driving. ETESS was demonstrated to perform in a manner similar to ECMS if applied to a HEV operated under charge-sustaining mode in terms of fuel economy, but with a very reduced computational effort [28].

In this work, the ETESS logic is extended to the management of a parallel plugin HEV. To this aim, an adaptive function is introduced, leading to an Adaptive ETESS strategy (named in the following as A-ETESS). The main aim of this work is to demonstrate the feasibility of the above strategy to the control of PHEV under CB mode, maintaining fuel economy levels similar to well-assessed strategies, such as Adaptive-ECMS (A-ECMS), with a computational effort similar to rule-based strategies. To this aim, the A-ETESS is implemented in a vehicle simulation model built on MATLAB/Simulink and tested along different driving cycles. The same adaptive function is introduced in the A-ECMS to benchmark the proposed control strategy in terms of fuel economy and computational effort. To compare the computational time, A-ETESS and A-ECMS are executed on the same MicroController Unit (MCU), ST Microelectronics board NUCLEO-H743ZI2, realizing processor-in-the-loop (PIL) tests, while the vehicle model is simulated on a PC-host.

Vehicle model and simulation platform

The investigated vehicle features a parallel P3 PHEV powertrain composed of a 3-cylinder spark ignition engine (ICE), an electric reversible machine (EM), a battery pack (BA), a DC-DC converter, a manual transmission (MT), and a torque coupler (TCP). The powertrain is schematized in Figure 1. Vehicle main characteristics are listed in Table 1.

Three modes, namely pure thermal mode, pure electric mode, and parallel mode are available to satisfy a tractive demand at the wheels. In pure thermal and pure electric mode, the demanded power is entirely provided by the engine and motor, respectively. Concerning the parallel mode, the power demand is provided in a combined manner by the engine and the motor.

The powertrain is schematized in a backward dynamic model of the PHEV under investigation, implemented in Matlab/Simulink. ICE fuel consumption and motor/generator efficiency are evaluated through speed-load lookup tables, here presented in Figure 2 and Figure 3, respectively. The battery module calculates the SoC of the battery pack, according to SoC-dependent internal resistance and open-circuit voltage.

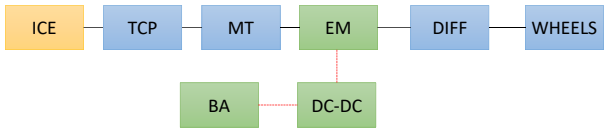

Figure 1. Powertrain schematic of tested PHEV.

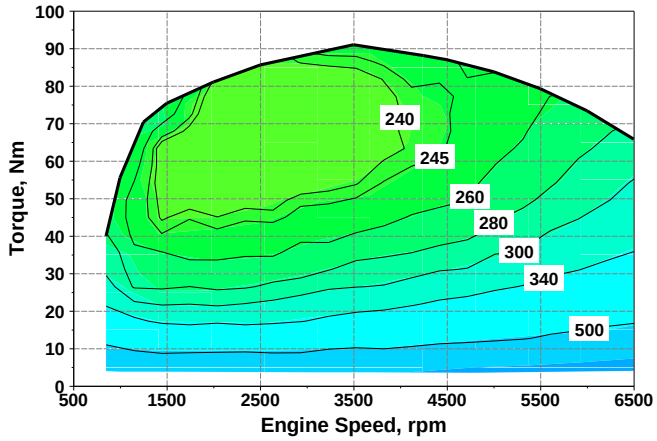

Figure 2. Engine BSFC map, g/kWh.

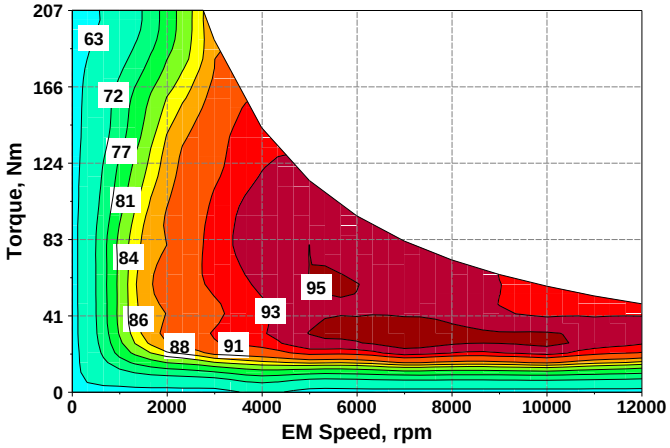

Figure 3. Electric machine efficiency map, %.

Table 1. Main characteristics of the tested PHEV

Plug-in Hybrid Electric Vehicle Features	
Vehicle	
Mass, kg	1100
Car aero drag, m^2	2.46
Wheel diameter, m	0.366
Axle ratio, -	3.32
Internal Combustion Engine	
Displacement, cm^3	999
Max Power, kW	46
Max Torque, Nm	90
Electric Machine	
Max Power, kW	60
Max Torque, Nm	207
Battery	
Rated Capacity, Ah	6.5
Gearbox	
Gear 1 Ratio, -	4.212
Gear 2 Ratio, -	2.637
Gear 3 Ratio, -	1.8
Gear 4 Ratio, -	1.386
Gear 5 Ratio, -	1
Gear 6 Ratio, -	0.772

Control strategies

In the next paragraphs, a brief description of ECMS and ETESS principles, suitable for HEV operated in charge sustaining mode is introduced. Subsequently, those strategies are extended at managing the PHEV in a charge blended mode. Note that in both ECMS and ETESS implementations a transmission control module is adopted. The desired gear is selected from a vehicle speed–accelerator pedal position lookup table to simplify the control logic and lower the computational effort.

Equivalent consumption minimization strategy

ECMS reduces the global energy minimization problem of HEVs to a local one. Its cost function is formulated as follow:

$$J = \dot{m}_f + s_0 \frac{P_{batt}}{LHV} \qquad (1)$$

It consists of an equivalent fuel rate, the sum of the actual fuel rate ($\dot{m}_f$) and a contribution related to the electric power, (where LHV is the fuel lower heating value and P_{batt} is the net electrical power as seen at the battery terminals), through an equivalence factor (s_0).

The equivalence factor represents the cost of the electric energy stored in the battery and its value for the optimal problem solution highly depends on vehicle characteristics and driving conditions. In the presented model ECMS implementation available in Powertrain Blockset Simulink library is taken as reference, following the formulation proposed by Onori et al. [27].

Efficient thermal electric skipping strategy

The ETESS strategy is based on an alternative utilization of the thermal engine and of the electric machine to satisfy the power demanded for the traction. Three operating modes can be defined: pure thermal mode, full electric mode, parallel mode. The choice between the thermal engine and electric motor depends, at each time, on the comparison between the actual fuel rate of the thermal engine, operating to fully satisfy the power demand, and an equivalent fuel rate related to the pure electric driving of the vehicle. The main concept behind the equivalent electric fuel rate lies in the idea that the power provided by the electric motor was produced by the thermal engine in an undefined time while working in its minimum brake specific fuel consumption $BSFC_{min}$. To take into account power losses along the driveline, power demand is corrected by efficiencies of driveline components. The equivalent fuel consumption is defined as:

$$\dot{m}_{f,el} = c_0 \cdot \frac{P_{dem} \cdot BSFC_{min}}{\eta_{diff}\,\eta_{EM}\,\eta_{GB}\,\eta_{batt}\,\eta_{inv}} \qquad (2)$$

where P_{dem} is the commanded wheel power, and η_{diff}, η_{EM}, η_{GB}, η_{batt}, η_{inv}, are respectively the efficiencies of the differential, electric motor, gearbox, battery, and inverter. c_0 is a tuning constant and represents the fuel-equivalent consumption of pure electric driving.

The actual fuel rate of the thermal engine depends on its operating point, defined by torque output and rotational speed:

$$\dot{m}_f = \frac{P_{dem} \cdot BSFC}{\eta_{GB}\eta_{diff}} \qquad (3)$$

Parallel mode is selected only if the thermal engine is not able to fully satisfy the power demand. In parallel mode, the thermal engine operates at its maximum load point and the electric motor delivers the lacking power to fulfill the demanded one.

Given the above definitions, ETESS can be summarized by the inequalities reported below:

$$\begin{cases} \dot{m}_f < \dot{m}_{f,eq} \Rightarrow \text{pure thermal mode} \\ \dot{m}_f > \dot{m}_{f,eq} \Rightarrow \text{pure electric mode} \end{cases}$$

Battery recharging is provided only through regenerative braking. In summary, ETESS can be considered as a specialization of ECMS for which the only allowed values for the power-split are either 0 or 1. ETESS advantage consists of reduced computational effort. In fact, the engine operating point depends only on tractive power demand, and a discrete exploration of power split is not needed.

Adaptive strategies

Adaptive variants of ECMS and ETESS are here realized according to a CB approach. In this context, the SoC target decreases linearly with the driven distance, following the equation:

$$\mathrm{SoC}_{target}(t) = \frac{\mathrm{SoC}_i - \mathrm{SoC}_{fin}}{\mathrm{L}_m} \cdot \left(\mathrm{L}_m - x(t)\right) + \mathrm{SoC}_{fin} \qquad (4)$$

where SoC_i and SoC_{fin} are respectively the SoC of the battery at the start and the end of the driving mission, $x(t)$ is vehicle position at time instant t and L_m is the total distance to be covered. It is worthwhile highlighting that the only information needed to evaluate the reference SoC are the initial state of charge of the battery (SoC_i), the desired SoC value at the end of the mission (SoC_{fin}), and the distance that vehicle must travel (that could be provided by a map service provider in real application on vehicle). In this paper, the ETESS, originally conceived to operate the powertrain in a charge sustaining mode, is extended for a CB strategy through the adaption of the tuning constant c_0 related to the weight of pure electric driving cost (Eq 3). The equivalent fuel consumption defined in Eq. (3) is reformulated as:

$$\dot{m}_{f,el} = k_{pen} \cdot c_0 \frac{P_{dem} \cdot BSFC_{min}}{\eta_{diff}\eta_{EM}\eta_{GB}\ \eta_{batt}\ \ \eta_{inv}} \qquad (5)$$

where the penalization factor k_{pen} is introduced. During the driving mission two scenarios are possible:

1) The actual SoC is higher than the reference SoC*. Pure electric driving must be promoted lowering the cost related to it.

2) The actual SoC is lower than the reference SoC*. Pure electric driving must be penalized raising the cost associated with it.

The term k_{pen} is distinguished for these scenarios. For this reason, two different functions are built depending on the difference between the actual SoC and the reference one SoC* and the normalized distance to travel ($\Delta x=(L_m-x)/L_m$). Logarithmic functions are selected to make the control strategy stable, and the correction of the adaptive cost is assumed to raise with the traveled distance and with the SoC error. For faster model running, the two functions are implemented in the form of a lookup table. Their values are shown in Figure 4 and Figure 5.

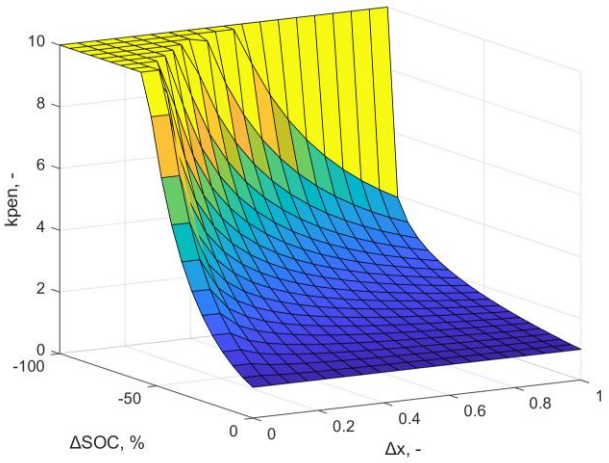

Figure 4. k_{pen} for SoC(x) < SoC*(x).

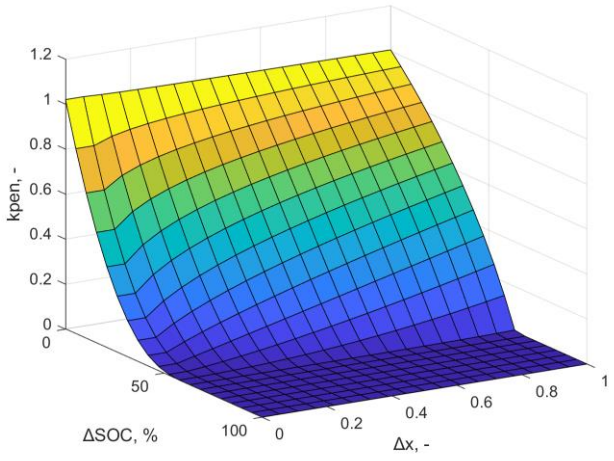

Figure 5. k_{pen} for SoC(x) > SoC*(x).

In order to have consistent comparisons, the adaptive term is introduced in the ECMS, leading to the following formulation:

$$J = \dot{m}_f + s_0 \cdot k_{pen} \cdot \frac{P_{batt}}{LHV} \qquad (6)$$

Preliminary tests on 5 driving cycles, namely WLTC, HWFET, ARTEMIS URBAN, JC08, and a Real Driving Cycle (RDC), showed that the proper values of c_0 and s_0 are slightly dependent on the driving mission. In those simulations, the c_0 and s_0 are selected by a trial-and-error procedure, where the monitored parameter to be minimized is the average difference between actual SoC and SoC_{target}. As an example, the SoC trends for optimal ($c_{0,opt}$ in black), and sub-optimal values of c_0 (0.95 in red and 1.15 in blue), and SoC_{target} (green) are depicted in Figure 6 for WLTC.

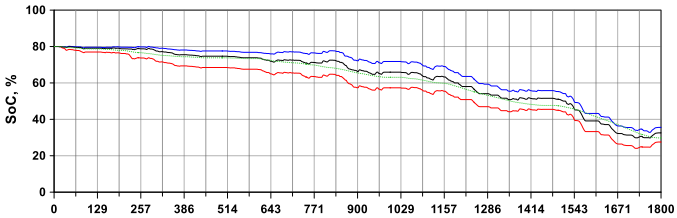

Figure 6. SoC along WLTC for: (black) c_0=1.05, (blue) c_0=1.15, (red) c_0=0.95, SoC* (green).

The cycle-dependent optimal values of c_0 and s_0 are then correlated to the travelled distance of each driving cycle, as shown in Figure 7. The latter also depicts appropriate fitting functions. Those functions will be used in the results presented in the following to assign the initial values of c_0 and s_0 whatever is the driving cycle, only as a function of the overall distance to be covered.

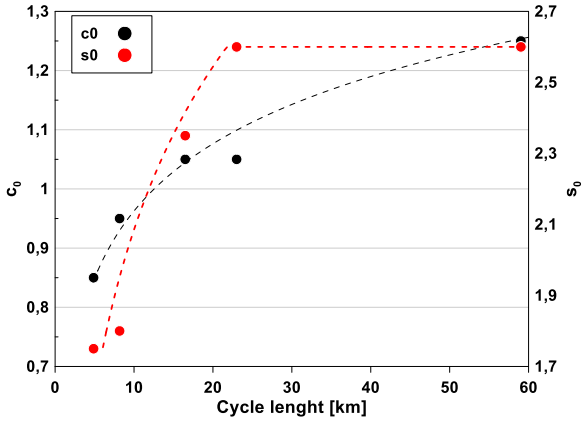

Figure 7. Driving cycle-tuned values of c_0 and s_0, and their fitting functions.

Test cases

A set of 10 driving cycles, listed in Table 2, have been selected for the comparison of A-ETESS and A-ECMS, with the aim of exploring their behavior under various scenarios, highly different in terms of maximum and mean speeds and accelerations, and distance to be covered.

An initial battery SoC of 80% and a final SoC of 30% have been specified, in compliance with typical plug-in hybrid operations.

To reinforce the validity of the comparisons, a Real Driving Emission-compliant cycle (RDE) and a Real Driving cycle, whose data have been collected from a GPS, have been considered (cycles # 9 and #10 in Table 2, respectively, plotted in Figure 8 e Figure 9).

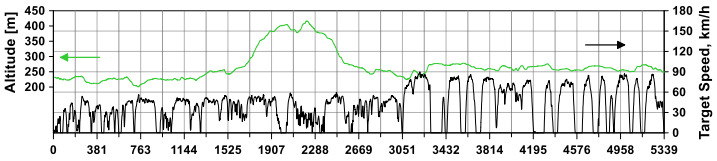

Figure 8. Real Driving Cycle: speed (black); altitude (green).

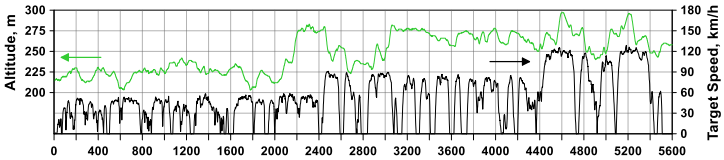

Figure 9. RDE Cycle: speed, (black); altitude, (green).

Fuel consumption correction related to battery discharge

In order to take into account the energy consumption related to battery discharge, typical of PHEV operations, a correction of the cumulated fuel consumed at the end of the driving mission has to be introduced. To this aim, the electrical energy globally used is converted into an equivalent mass of fuel on the basis of the following hypothesis. The energy taken from the battery (ΔE_{batt}) is assumed to have been produced by the engine operating at its average efficiency point ($\bar{\eta}$). The correction of the fuel mass (Δm_{eq}) can hence be represented as follow:

$$\Delta m_{eq} = \frac{\Delta E_{batt}}{LHV \cdot \bar{\eta}} \qquad (7)$$

The total fuel consumed (m_{tot}) to cover the driving mission is expressed as:

$$m_{tot} = m_{ICE} + \Delta m_{eq} \qquad (8)$$

where m_{ICE} is the actual mass of fuel consumed by the ICE. The total fuel consumed, normalized by the travelled distance along the driving mission, will be adopted in the following section as an indicator of vehicle fuel economy.

Table 2. Tested driving cycles.

TC	Cycle	L_m	V_{mean}	a_{max}	V_{max}
	units	km	km/h	m/s^2	km/h
1	WLTC	23.00	46.5	1.75	131.3
2	FTP75	17.77	25.9	1.48	91.2
3	HWFET	16.49	77.6	1.43	96.4
4	LA92	15.80	39.6	3.08	108.1
5	ARTEMIS URBAN	4.87	17.7	2.86	57.7
6	ARTEMIS RURAL	17.27	57.5	2.36	111.5
7	ARTEMIS HIGH 130	28.74	96.9	1.92	131.8
8	JC08	8.171	24.4	1.69	81.6
9	RDC	59.02	39.8	3.33	89.9
10	RDE	78.85	50.7	5.04	128.8

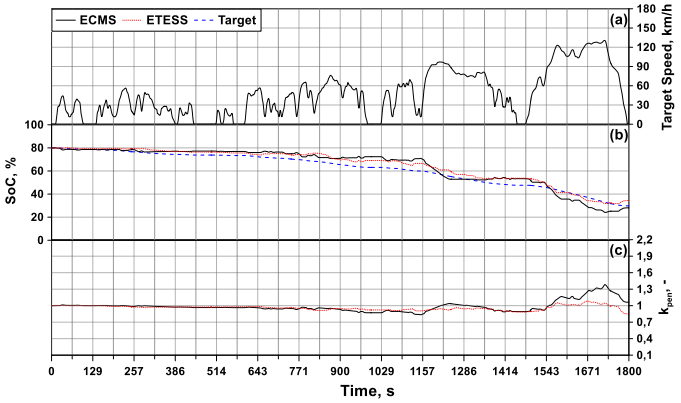

Figure 10. WLTC, (a) Target speed. ETESS/ECMS comparisons of battery SoC (b) and k_{pen} (c).

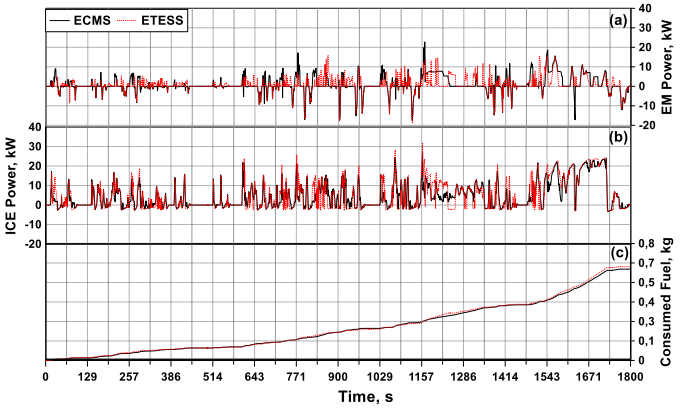

Figure 11. WLTC, ETESS/ECMS comparisons of EM power (a), ICE power (b), and cumulated consumed fuel (c).

Results

For sake of brevity results for test cases 1, 5, 8, 10, (representative for a high-speed cycle, low-medium speed cycles, and a RDE-compliant cycle) are discussed in detail below.

Starting the discussion from test case 1, both A-ECMS and A-ETESS prove to follow the SoC target profile and almost reach the desired SoC at the end of the mission (Figure 10-b). The adaptive term properly reflects the error between the instantaneous SoC and the instantaneous target SoC (Figure 10-c).

However, ETESS results present more skip between engine ON/OFF, resulting possibly in worse drivability in a real vehicle application (Table 3). Maximum and mean vehicle acceleration rates, and ICE skip number, reported in Table 3, are considered as indicators of vehicle drivability.

During the high-speed portion of the cycle, between 1400 and 1800s, the EM supports the ICE, which delivers its maximum torque to fulfill the power demand at the wheels both in A-ECMS and A-ETESS. This is also evidenced by similar SoC trends (Figure 11-b). Globally, the considered strategies behave in a very similar manner, leading to analogous levels of consumed fuel (Figure 11-c).

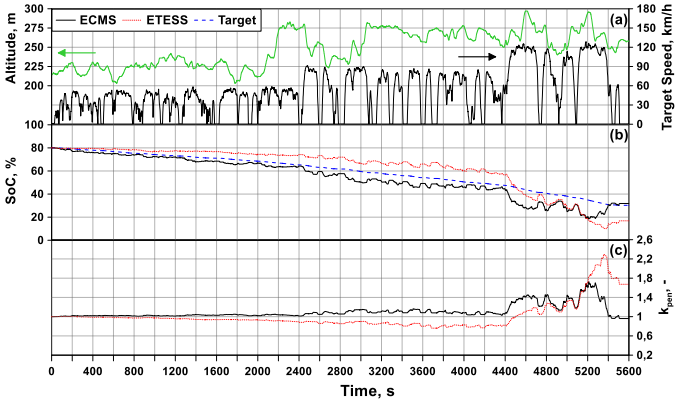

Figure 12. RDE, (a) Target speed. ETESS/ECMS comparisons of battery SoC (b) and k_{pen} (c).

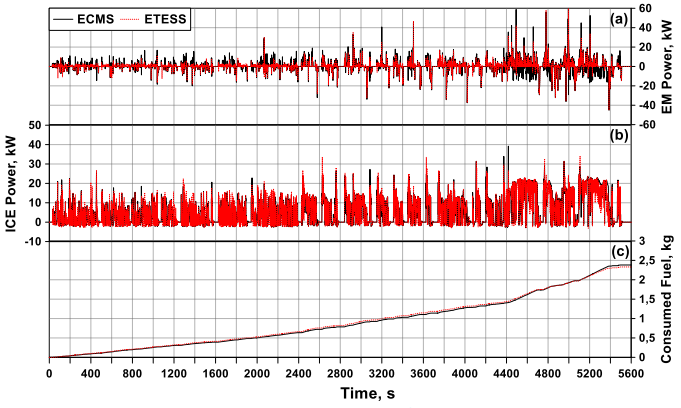

Figure 13. RDE, ETESS/ECMS comparisons of EM power (a), ICE power (b), and cumulated consumed fuel (c).

In Figure 12, the instantaneous trends of SoC (Figure 12-b), and the adaptive term (Figure 12-c) along the RDE-compliant cycle are depicted (test case #10 of Table 2). Moreover, the comparisons of ICE and EM powers and consumed fuel are reported in Figure 13. Soc ends and EM powers highlight significant differences in electrical energy usage between the two strategies due to the possibility of A-ECMS exploring intermediate power split. During the low-speed part of the cycle, A-ETESS prefers pure thermal mode more frequently than A-ECMS. In the portion of the cycle between 4400 and 5400s, A-ECMS can recharge the battery keeping ICE mainly on its maximum torque working point. In A-ETESS, instead, battery recharge during traction is not possible and the ICE only delivers the power needed for traction. Consequently, when the EM is forced to fulfill power demand in parallel mode, this leads to a quite deep battery discharge, reaching a 16% SoC at the end of the cycle. Despite those limitations of A-ETESS, the cumulated fuel consumed is lower than the A-ECMS counterpart. On the other hand, a substantially greater electric energy consumption emerges overall. Those results globally compensate each other, leading, as shown in the following, to similar fuel economies. It is worthwhile mentioning that an enhanced gear shifting strategy and a more powerful ICE could significantly improve A-ETESS behavior.

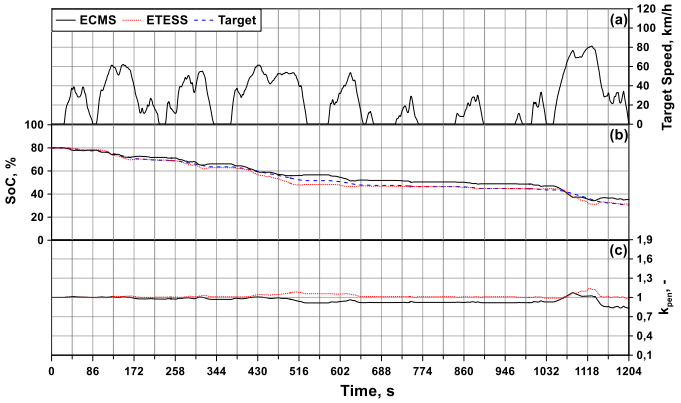

Figure 14. JC08, (a) Target speed. ETESS/ECMS comparisons of battery SoC (b) and k_{pen} (c).

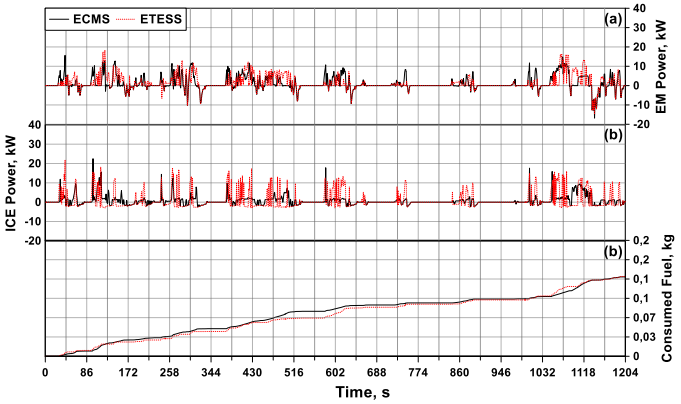

Figure 15. JC08, ETESS/ECMS comparisons of EM power (a), ICE power (b), and cumulated consumed fuel (c).

To show the capability of the A-ETESS to deal with slow and short driving cycles, in Figure 14 and Figure 15, comparisons with A-ECMS along the JC08 cycle are depicted (test case #8 of Table 2). The adaptive term is always next to the unit (Figure 14-c) and the trends of the SoC are quite close to the target (Figure 14-b). The final consumed fuels, applying A-ECMS and A-ETESS, are similar but the first involves a greater battery discharge at the cycle end, leading to a worse fuel economy. As better detailed in the following, this is due to some issues in the management of ICE when this is operated with a null-load.

Table 3. Engine ON/OFF number and maximum and mean value of vehicle acceleration derivative for test cases 1,5,8,10.

TC	Strategy	Engine ON/OFF, -	$max\left(\frac{da}{dt}\right), \frac{m}{s^3}$	$mean\left(\left\|\frac{da}{dt}\right\|\right), \frac{m}{s^3}$
1	A-ETESS	238	1.253	0.145
	A-ECMS	156	1.329	0.133
5	A-ETESS	120	2.151	0.331
	A-ECMS	152	2.132	0.332
8	A-ETESS	170	1.008	0.150
	A-ECMS	135	1.354	0.137
10	A-ETESS	1324	2.363	0.200
	A-ECMS	856	2.385	0.195

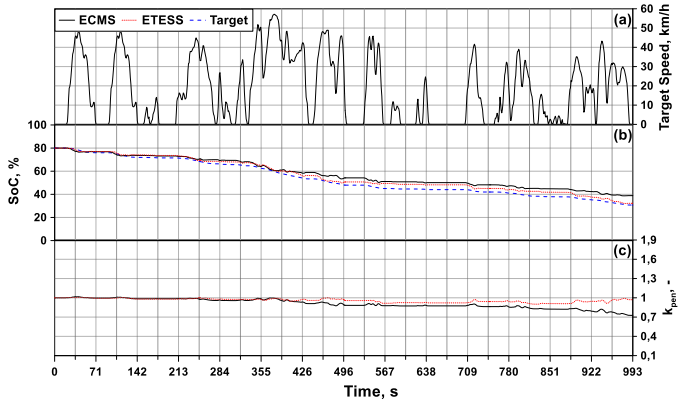

Figure 16. Artemis Urban, (a) Target speed. ETESS/ECMS comparisons of battery SoC (b) and k_{pen} (c).

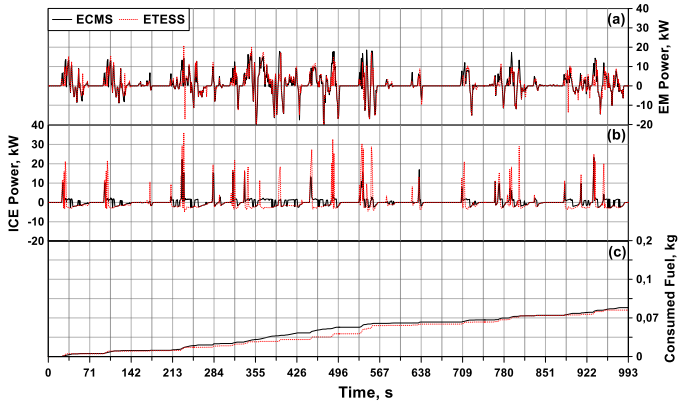

Figure 17. Artemis Urban, ETESS/ECMS comparisons of EM power (a), ICE power (b), and cumulated consumed fuel (c).

Detailed results for Artemis Urban Cycle (test case #8 of Table 2) are depicted in Figure 16 and Figure 17. A-ETESS and A-ECMS differently manage ICE and EM as highlighted in Figure 17-a and Figure 17-b, respectively. In the case of A-ETESS, the EM delivers a greater power when the ICE is operated load-less (null torque request) and the torque converter continues transmitting power (negative) to the driveline. In those circumstances, the battery quickly discharges as shown in Figure 16-b. The ICE works less frequently, even if at higher loads, and hence with higher efficiencies. The overall fuels consumed at the cycle end of A-ETESS and A-ECMS are similar (Figure 17-c), but a lower final SoC level is reached in the first case. This, as shown in the following, will determine a remarkable worsening of fuel economy in the comparison between A-ETESS and A-ECMS.

In the future development of this activity, the adoption of detailed clutch control, combined with the removal of the torque converter, is expected to speed-up the ICE engagement / disengagement, and to nullify the dissipations related to ICE load-less operations. This is expected to align fuel economy performance of A-ETESS with respect to A-ECMS one.

A global synthetic comparison between the results of the two strategies is realized through the bar charts in Figure 18. They represent the total fuel consumed per kilometer, for A-ETESS and A-ECMS, and over each couple of bars is shown the percentage difference, evaluated as:

$$\Delta m_{tot} = \frac{m_{tot}^{A-ECMS} - m_{tot}^{A-ETESS}}{m_{tot}^{A-ECMS}} \cdot 100 \qquad (9)$$

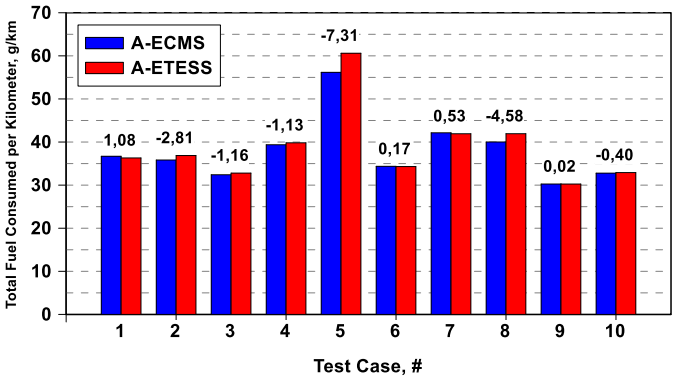

Figure 18. Comparison between A-ETESS and A-ECMS of kilometric total consumed fuel and percent difference in the test cases of Table 2.

As it can be observed, the average total fuel consumed difference between A-ETESS and A-ECMS is below 2% and in most cases of about 1% or lower. Greater differences emerge only for test cases # 5 and #8, for the issues related to load-less ICE operations above mentioned. From the viewpoint of vehicle drivability, no relevant difference emerges between A-ETESS and A-ECMS, as evidenced by maximum and averaged values of vehicle acceleration derivative reported in Table 3. As expected, A-ETESS involves a greater number of engine ON/OFF than A-ECMS in most of the test cases of Table 3, even if for case # 5 the opposite situation verified. The consequences of such circumstance of course would require some verification in a real on-vehicle application, especially in terms of thermal management and effectiveness of aftertreatment devices of the ICE.

PIL Test

In this section PIL tests' results are presented. The execution of A-ETESS and A-ECMS are tested on the NUCLEO-H743 [29]. It is a high-performance board for optimized control, equipped with an ARM Cortex-M7 running up to 480 MHz, 424 Core-Mark / 1027 DMIPS executing from Flash memory. The objective of the PIL test is to evaluate the execution time and computational effort of the C-Code generated for running on the NUCLEO-H743. The PIL testing procedure is based on asynchronous serial communication between the NUCLEO board and PC-Host. To this aim, Simulink Coder for STMicroelectronics NUCLEO board is used. At the end of the simulation in PIL mode, Simulink generates the code execution profiling report. Results are similar for each test case in Table 2, so for sake of brevity, only WLTC results are reported in Table 4. The latter shows that A-ETESS is two orders of magnitude faster than A-ECMS, with a maximum CPU Utilization of 0.015% in the place of 22.95%. For both strategies, the average execution time is lower than the typical cycle time of a CAN message for an updated engine torque request (10 ms), but A-ETESS reduced computational effort confirm the possibility to run multiple control strategy on the same micro-controller optimizing its utilization.

Table 4. PIL testing results for WLTC

Task	A-ETESS	A-ECMS	Difference, %
Maximum CPU Utilization, %	0.015	22.95	-99.93
Average CPU Utilization, %	0.005	14.31	-99.96
Maximum Execution Time, ms	0.030	2.29	-98.68
Average Execution Time, ms	0.011	1.43	-99.22

Conclusions

This paper describes the extension of a simplified control strategy, named A-ETESS, for plug-in hybrid electric vehicles. It is developed for different driving cycles in a vehicle model built in Matlab/Simulink environment. A-ETESS is a charge-blended control strategy in which desired SoC target decrease linearly with the driven distance. The fundamental concept of the ETESS, based on an alternative utilization of the thermal and electric unit to fulfill the power demand of the vehicle, is extended through the implementation of an adaptive term. It is based on logarithmic functions, selected to make the strategy stable, and it is implemented in the form of a two-dimensional look-up table. To benchmark the proposed control strategy in terms of fuel consumption and computational effort, the same adaptive function is introduced in the ECMS (A-ECMS).

In a preliminary stage, the proper value of c_0 and s_0, respectively the weight of electric energy cost in ETESS and the equivalence factor in ECMS, are selected to minimize the average difference between actual SoC and SoC_{target} for 5 driving cycles, namely WLTC, HWFET, ARTEMIS URBAN, JC08, RDC. With appropriate fitting functions, c_0 and s_0 optimal values are then correlated to the travelled distance to generalize the approach to any driving cycle. The fitting function is used to assign the initial value of c_0 and s_0, whatever is the driving cycle. The results of the test cases point out that the average total fuel consumption difference between A-ETESS and A-ECMS is below 2%.

To verify the possibility of A-ETESS to be implemented in a real-time vehicle application, and to compare the computational time, A-ETESS and A-ECMS are executed on the NUCLEO-H743, realizing PIL tests, while the vehicle model is simulated on a PC-host. PIL results confirmed that A-ETESS is two orders of magnitude faster than A-ECMS and its average execution time is lower than the typical cycle time of a CAN message for an updated engine torque request. At the expense of slightly worse fuel consumption, the proposed strategy greatly reduces computational costs.

As a future development of this work, the proposed methodology for the estimation of c_0 will be refined to improve A-ETESS performance when it is implemented for a connected and autonomous vehicle. Vehicle connectivity can provide information to train neural networks which can cooperate with the proposed strategy. A detailed clutch model to disengage ICE, in the case of load-less operations, and an enhanced gear shifting strategy will be introduced, as well.

Contact Information

References

1. Zhang, F., Wang, L., Coskun, S., Pang, H., Cui, Y., Xi, J., "Energy Management Strategies for Hybrid Electric Vehicles: Review, Classification, Comparison, and Outlook," Energies 13(13):3352, 2020, doi:10.3390/en13133352.
2. Rizoulis, D., Burl, J., Beard, J., "Control strategies for a series-parallel hybrid electric vehicle," SAE Technical Paper 2001-01-1354, 2001, doi:10.4271/2001-01-1354.
3. Sharer, P., B., Rousseau, A., Karbowski, D., Pagerit, S., "Plug-in hybrid electric vehicle control strategy: comparison between

EV and charge-depleting options," SAE Technical Paper 2008-01-0460, 2008, doi:10.4271/2008-01-0460.
4. Powell, B., K., Bailey, K., E., Cikanek, S., R., "Dynamic modeling and control of hybrid electric vehicle powertrain systems," *IEEE Control System Magazine*,18(5):17–33, 1998, doi:10.1109/37.722250.
5. Brahma, A., Guezennec, Y., Rizzoni G., "Optimal energy management in series hybrid electric vehicles," *Proceedings of the 2000 American control conference*, 1: 60–64, 2000, doi:10.1109/ACC.2000.878772.
6. Lin, C., C., Kang, J., M., Grizzle, J., W., Peng, H., "Energy management strategy for a parallel hybrid electric truck," *Proceedings of the 2001 American control conference*, 4:2878–2883, 2001, doi:10.1109/ACC.2001.946337.
7. Mansour, C., Clodic, D., "Optimized energy management control for the Toyota hybrid system using dynamic programming on a predicted route with short computation time," *International Journal of Automotive Technology*, 13(2):309−324, 2012, doi:10.1007/s12239−012−0029−0.
8. Xie, S., Li, H., Xin, Z., Liu, T.,Wei, L., "A pontryagin minimum principle-based adaptive equivalent consumption minimum strategy for a plug-in hybrid electric bus on a fixed route," *Energies*, 10(9):1379, 2017, doi:10.3390/en10091379.
9. Ghasemi, M., Song, X., "A computationally efficient optimal power management for power split hybrid vehicle based on pontryagin's minimum principle," *Proceedings of the ASME 2017 Dynamic Systems and Control Conference*, 2, 2017, doi:10.1115/DSCC2017-5244.
10. Kang, C., Song, C., Cha, S., "A costate estimation for pontryagin's minimum principle by machine learning," *Proceedings of the 2018 IEEE Vehicle Power and Propulsion Conference*, 1–5, 2018, doi:10.1109/VPPC.2018.8604982.
11. Zhang, J., Zheng, C., Cha, S.W., Duan, S., "Co-state variable determination in pontryagin's minimum principle for energy management of hybrid vehicles," *International Journal of Precision Engineering and Manufacturing*, 17(9):1215–1222, 2016, doi:10.1007/s12541-016-0146-1.
12. N., W., Kim, D., H., Lee, C., Zheng, C. Shin, H., Seo, S., W, Cha, 2013. "Realization of PMP-based control for hybrid electric vehicles in a backward-looking simulation," *International Journal of Automotive Technology*, 15(4):625−635, 2014, doi:10.1007/s12239−014−0065−z.
13. Paganelli, G., Delprat, S., Guerra, T., M., Rimaux, J., Santin, J., J., "Equivalent consumption minimization strategy for parallel hybrid powertrains," *Proceedings of the Vehicular Technology Conference*, 4:2076-2081, 2002, doi:10.1109/VTC.2002.1002989.
14. Nüesch, T., Cerofolini, A., Mancini, G., Cavina, N., Onder, C., Guzzella, L., "Equivalent consumption minimization strategy for the control of real driving nox emissions of a diesel hybrid electric vehicle," *Energies*, 7:3148–3178, 2014, doi:10.3390/en7053148.
15. Wang, J., Wang, Q., Wang, P., Zeng, X., "The Development and Verification of a Novel ECMS of Hybrid Electric Bus," *Mathematical Problems in Engineering*, 2014, doi:10.1155/2014/981845.
16. Gonder, J., and Markel, T., "Energy Management Strategies for Plug-In Hybrid Electric Vehicles," SAE Technical Paper 2007-01-0290, 2007, doi:10.4271/2007-01-0290.
17. Zhang, B., Mi, C., C., and Zhang, M., "Charge-Depleting Control Strategies and Fuel Optimization of Blended-Mode Plug-In Hybrid Electric Vehicles," *IEEE Transactions on Vehicular Technology*, 60(4):1516-1525, 2011, doi:10.1109/TVT.2011.2122313.
18. Alipour, H., and Asaei, B., "A heuristic power management strategy for plug-in hybrid electric vehicles," *2011 2nd International Conference on Electric Power and Energy Conversion Systems*, 1-6, 2011, doi:10.1109/EPECS.2011.6126803.
19. Peng, J., He, H., Xiong, R., "Rule based energy management strategy for a series–parallel plug-in hybrid electric bus optimized by dynamic programming," *Applied Energy*, 185(2):1633-1643, 2017, doi:10.1016/j.apenergy.2015.12.031.
20. Tribioli, L., M., Capata, R., Sciubba, E., Jannelli, E., Bella, G., "A Real Time Energy Management Strategy for Plug-in Hybrid Electric Vehicles based on Optimal Control Theory," *Energy Procedia*, 45:949-958, 2014, doi:10.1016/j.egypro.2014.01.100.
21. Shankar, R., Marco, J., Assadian, F., "Design of an Optimized Charge-Blended Energy Management Strategy for a Plug-in Hybrid Vehicle," *Proceedings of the UKACC International Conference on Control*, 1:619-624, 2012, doi:10.1109/CONTROL.2012.6334701.
22. Capancioni, A., Brunelli, L., Cavina, N., Perazzo, A., "Development of Adaptive-ECMS and predictive functions for Plug-in HEVs to Handle Zero-Emission Zones Using Navigation Data," SAE International, Conference Proceedings, 2021-09-05, doi:10.4271/2021-24-0105.
23. Denis, N., Dubois, M., R., Dubé, R., et al. "Blended Power Management Strategy Using Pattern Recognition for a Plug-in Hybrid Electric Vehicle," *International Journal of Intelligent Transportation Systems Research*, 14(2):101-114, 2016, doi:10.1007/s13177-014-0106-z.
24. Wang, S., Huang, X., López, J., M., Xu, X., and Dong, P., "Fuzzy Adaptive-Equivalent Consumption Minimization Strategy for a Parallel Hybrid Electric Vehicle," *IEEE Access*, 7:133290-133303, 2019, doi:10.1109/ACCESS.2019.2941399.
25. Shaobo, X., Xiaosong, H., Shanwei, Q., Kun, L., "An artificial neural network-enhanced energy management strategy for plug-in hybrid electric vehicles," *Energy*, 163:837-848, 2018, doi:10.1016/j.energy.2018.08.139.
26. Onori, S., Tribioli, L., "Adaptive Pontryagin's Minimum Principle supervisory controller design for the plug-in hybrid GM Chevrolet Volt," *Applied Energy*, 147:224-234, 2015, doi:10.1016/j.apenergy.2015.01.021.
27. Onori, S., Serrao, L., and Rizzoni, G., "Hybrid Electric Vehicles Energy Management Systems" (New York, Springer, 2016) ISBN: 978-1-4471-6779-2.
28. De Bellis, V., Malfi, E., Tufano, D., and Bozza, F., "Efficient Thermal Electric Skipping Strategy Applied to the Control of Series/Parallel Hybrid Powertrain," SAE Technical Paper 2020-01-1193, 2020, doi:10.4271/2020-01-1193.
29. ST Microelectronics. STM32H7 Nucleo-144 Boards (MB1364); ST Microelectronics: Santa Clara, CA, USA, 2020.

Acronyms

A-ECMS	Adaptive - ECMS
BA	Battery pack
BSFC	Brake Specific Fuel Consumption
CB	Charge Blended
CD	Charge Depleting
CS	Charge Sustaining
DP	Dynamic Programming
ECMS	Equivalent Consumption Minimization Strategy
EM	Electric motor
EM	Electric machine

EMS	Energy Management Strategy
ETESS	Efficient Thermal / Electric Skipping Strategy
FC	Fuel consumption
HEV	Hybrid electric vehicle
HIL	Hardware in the Loop
ICE	Internal Combustion Engine
LHV	Lower Heating Value
MT	Manual Transmission
PHEV	Plug-in HEV
PIL	Processor in the Loop
PMP	Pontryagin Minimum Principle
RDC	Real Driving Cycle
RDE	Real driving Emission
SoC	State of charge

Symbols

m	mass
ΔE_{batt}	Battery energy variation
$\dot{m}_f$	Fuel mass rate
s_0	Equivalence factor
k_{pen}	Adaptive term
P_{batt}	Battery Power

Greeks

η	Efficiency

Subscripts

a	Acceleration
batt	Battery
dem	Demanded
diff	Differential
eq	Equivalent
f	Adaptive - ECMS
fin	Final
GB	Gear-box
i	Initial
inv	Inverter
m	Mission
max	Maximum
min	Minimum
tot	Total
v	Velocity

Superscripts

*	Target
-	Mean Value